Selective Sorption of Heavy Metal on Phosphorylated Sago Starch-Extraction Residue

Masato Igura,[1] Masanori Okazaki[2]

[1]*Graduate School of Bio-Applications and Systems Engineering, Tokyo University of Agriculture and Technology, 2-24-16, Koganei, Tokyo 184-8588, Japan*
[2]*Institute of Symbiotic Science and Technology, Tokyo University of Agriculture and Technology, 2-24-16, Koganei, Tokyo 184-8588, Japan*

Received 25 February 2011; accepted 14 May 2011
DOI 10.1002/app.34899
Published online 5 October 2011 in Wiley Online Library (wileyonlinelibrary.com).

ABSTRACT: The phosphorylated sago starch-extraction residue (P-SR) was produced for the removal of heavy metal from wastewater. The phosphoric ester in the phosphorylated residue was evaluated by means of infrared microspectrometry and solid-state NMR. In this study, the phosphorus contents of produced P-SR, phosphorylated cellulose (P-C), and phosphorylated sago starch were 31.7, 34.2, and 4.6 mg/g, respectively. The phosphorus contents of P-C and sago starch were clearly different because of the difference of each structure. The maximum sorption capacities of heavy metals (cadmium, lead, copper, and zinc) in single heavy metal sorption on P-SR were 0.20, 0.25, 0.36, and 0.24 mmol/g (Cu > Pb > Zn > Cd), respectively. On the other hand, the amount of sorbed heavy metals in coexisted heavy metal sorption on P-SR followed the order of Pb > Cu > Cd > Zn that was different from the relations of maximum sorption capacities for individual heavy metals. The heavy metal sorption behavior in single and coexisted heavy metal solution for P-SR were different and P-SR showed the intrinsic heavy metal sorption affinity, called as selective sorption. © 2011 Wiley Periodicals, Inc. J Appl Polym Sci 124: 549–559, 2012

Key words: adsorption; esterification; surface modification

INTRODUCTION

Severe environmental regulations in the world require the treatment of wastewater to remove heavy metal.[1–4] Several remediation techniques, such as precipitation on lime,[5] ion exchange,[6–8] adsorption onto activated carbon,[9,10] membrane processes,[11] and electrolytic methods,[12] have been utilized to reduce the concentration of heavy metal ions in effluents.[13] However, these methods are generally expensive for the application in the environment. The most common metals found in wastewater are copper, cadmium, nickel, lead, and zinc that are toxic at high concentration.[14]

The sago palm (*Metroxylon sagu*) has a potential to yield up to 25 tons of starch per hectare per year, and the sago starch yield per unit area could be about 3–4 times that of rice, corn, and wheat and about 17 times that of cassava.[15] Thus, sago starch is a staple food in tropical Southeast Asia. It is a promising solution for the food crisis of countries with tropical wetlands and may also further their economical development. However, during the starch extraction, large amounts of residue that has no suitable method of disposal are produced in sago starch producing countries in Southeast Asia.

Recently some of the effective use of biological waste materials; such as rice straw, bagasse cotton stalk, and wood pulp have been reported.[16–18] Sago starch-extraction residue was used for the raw material of the production of biodegradable plastics,[19,20] the heavy metal sorbent,[21] and other additional uses that are desirable.

The effective sorbent with chemical modification of agricultural by-products[17,18,22–27] is the techniques to generate efficient, low-cost sorbents for the removal of heavy metal from water. The sago starch-extraction residue could be treated in some way to make it an effective sorbent,[21] which could be used for removal of heavy metals in wastewater. Phosphorylation, which is an esterification reaction, can be expected to impart heavy metal sorption capacity to sago starch-extraction residue.

In a previous study, the sago starch-extraction residue phosphorylated using phosphoryl chloride was produced to investigate the cadmium sorption from waste water.[22]

The objectives of this study are to evaluate the selective sorption affinity of heavy metals to phosphorylated sago starch-extraction residue (P-SR) under the coexisting ions.

Correspondence to: M. Igura (mst_igr@yahoo.co.jp).

MATERIALS AND METHODS

Phosphorylation of sago starch-extraction residue

Phosphorylation for sago starch-extraction residue was carried out according to the methods of Igura and Okazaki.[21] Sago starch-extraction residue obtained from Leyte in the Philippines was used as a raw material. The extraction residue was pulverized in a grinder and passed through a 0.5-mm sieve. After lipid removal[19] and drying, the extraction residue and *N*,*N*-dimethylformamide were mixed, and then phosphoryl chloride (5 mL) was added, along with tributylamine. Then, the slurry was stirred in an oil bath at 80°C for 2 h. After the reaction, the product was washed with ethanol-hexane (9 : 1) solution. The phosphorylated extraction residue (powder) was designated as P-SR. Most of sago starch-extraction residue is composed of remaining starch and cellulose, and it also contains hemicellulose and lignin.[28] Thus, the sago starch and cellulose are main components of sago starch-extraction residue. The phosphorylated sago starch (P-SS) and cellulose were also prepared from the pure sago starch and cellulose for comparison with the heavy metal sorption behavior of P-SR. Tsujimoto et al.[29] reported that the particle size (in major axis) of sago starch ranged from 30 to 45 μm. Thus, the sago starch, which was passed through a 45-μm sieve, was used for the production of the P-SS, and the microcrystalline cellulose (Avicel, E. Merck, Darmstadt, Germany, particle size $\leq$ 50 μm) was used for the production of the phosphorylated cellulose (P-C).

Elemental analysis

Phosphorus analysis

The phosphorus contents of the untreated sample (sago starch-extraction residue, microcrystalline cellulose, and sago starch) and the phosphorylated sample (P-SR, P-C, and P-SS) were determined by the molybdenum blue method.[21,30,31] After the pretreatment of the samples, the molybdenum blue reagent was added into the resulting solution, and the phosphorus contents of samples were determined with a spectrophotometer (BioSpec-1600, Shimadzu Co.) by means of the colorimetric method.

Total carbon and total nitrogen analysis

The total carbon and total nitrogen contents of the P-SR, P-C, P-SS, and the untreated sago starch-extraction residue (hereafter untreated extraction residue) were determined with a CN coder (MT-700, Yanaco Co.).[32] The P-SR (0.2 g) was mixed with 5 g of copper oxide, and the mixture was placed in the platinum sample holder and combusted in the oxidation furnace of the CN coder. The P-C, P-SS, and the untreated extraction residue were also subjected to the same procedure. Hippuric acid [carbon (60.33%) and nitrogen (7.82%)] was used as a standard for total carbon and nitrogen analysis.

Infrared microspectrometric analysis of P-SR

Fourier transform infrared (FT-IR) analysis of P-SR was carried out with an IR microspectrometer (FT/IR-4100 type A and IRT-3000, JASCO Co.) and a KBr disk with an aliquot of P-SR. The sago starch and the fiber in P-SR were selected by IR microspectrometer and they were analyzed in the wavenumber range of 600–4000 cm^{-1}. P-C, P-SS, and the untreated extraction residue were subjected to the same procedure.

^{31}P and ^{13}C solid-state NMR analysis

^{31}P and ^{13}C solid-state CP/MS NMR analyses of P-SR, P-C, P-SS, and the untreated extraction residue were carried out with a solid-state NMR spectrometer (NM-ECX, JEOL Co.). P-SR powder was placed in a zirconia sample tube. The prepared sample tube was used for both ^{13}C and ^{31}P solid-state NMR analysis. The ^{31}P NMR conditions were as follows: resonance frequency 500 MHz, spinning rate 10 kHz, number of points 2048, and number of scans 512 at 25°C. Ammonium phosphate dibasic [$(NH_4)_2HPO_4$] was used as a standard for ^{31}P. The ^{13}C-NMR conditions were as follows: resonance frequency 500 MHz, spinning rate 10 kHz, number of points 2048, and number of scans 1024 at 25°C. Adamantine ($C_{10}H_{16}$) was used as a standard for ^{13}C.

Heavy metal sorption on P-SR

Cadmium sorption on P-SR, P-C, and P-SS

The different dose of P-SR (0.05–0.20 g) was stirred with 25 mL of aqueous cadmium (50 mg/L) at pH 4.0 for 1 h (in duplicate). The supernatant was filtered by No. 5C (Advantec) filter paper and 0.45-μm membrane filter, and the concentration of heavy metal ions in the filtrate was determined with an atomic absorption spectrophotometer (Z-5010, HITACHI.). The amount of sorbed heavy metal on P-SR was calculated from the amount of remaining heavy metal ions in the filtrate. The sorption data were fitted to a Langmuir isotherm:

$$C_e/q_e = 1/(bQ_{\max}) + C_e/Q_{\max}$$

where C_e is the concentration of the cadmium at equilibrium (mg/L), q_e is the amount of sorbed cadmium at equilibrium (mg/g), b is a constant related to the energy of sorption, and $Q_{\max}$ is the maximum

TABLE I
Phosphorus Content of P-SR Sample

Sample	Phosphorus mg P/g DW	Total carbon g/g DW	Total nitrogen g/g DW	Phosphate ester percentage (%)
P-SR[a]	31.7	0.40	0.01	6.1
Untreated[b]	0.0	0.41	0.00	–
P-C[c]	34.2	0.43	0.01	6.3
Microcrystalline cellulose	0.0	0.42	0.01	–
P-SS[d]	4.6	0.43	0.01	0.9
Sago starch[e]	0.0	0.43	0.01	–

DW: Dry weight.
[a] Phosphorylated sago starch-extraction residue.
[b] The untreated sago starch-extraction residue.
[c] Phosphorylated microcrystalline cellulose.
[d] Phosphorylated sago starch.
[e] The sago starch that was passed through a 45-μm sieve.

sorption capacity for cadmium (mg/g). The P-C and P-SS were also subjected to the same procedure.

Selectivity for the heavy metal sorption on P-SR

For the evaluation of the selectivity for the heavy metal sorption on P-SR, single heavy metal sorption using cadmium (Cd), lead (Pb), copper (Cu), and zinc (Zn) was conducted. The maximum sorption capacity of cadmium, lead, copper, and zinc for P-SR was determined. Meanwhile, competitive heavy metal sorption that contained cadmium, lead, copper, and zinc was also conducted for the evaluation of the sorption affinity for the heavy metals on P-SR. Many kinds of metal ions coexist in the actual field environment.[33] Therefore, the sorption test of mixed metal ions on P-SR is necessary for the field applications of P-SR.

Maximum sorption capacity of single heavy metal

The different dose of P-SR (0.025–0.20 g) was dispersed individually in 25 mL of aqueous for cadmium (50 mg/L), lead (100 mg/L), copper (50 mg/L), and zinc (50 mg/L) at pH 4 for 1 h, respectively, (in duplicate). The amounts of sorbed heavy metal ions on P-SR were determined according to the method described in section of cadmium sorption.

Selective sorption capacity under coexisting heavy metals

Selective heavy metal sorption that contained cadmium, lead, copper, and zinc was also conducted for the evaluation of the sorption affinity for the heavy metals on P-SR. The mixed heavy metal solution (25 mL, pH 4.0) that included the 0.2 mmol/L of cadmium, lead, copper, and zinc, was prepared. P-SR (0.05 g) was dispersed in 25 mL of mixed heavy metal solution at pH 4 for 1 h. The amounts of sorbed heavy metal ions on P-SR were determined according to the method described in section of cadmium sorption.

RESULTS AND DISCUSSION

Elemental characteristics of P-SR

Table I shows the phosphorus content of P-SR, P-C, P-SS, and the untreated extraction residue. The phosphorus content of P-SR (31.7 mg P/g) due to the introduction of phosphorus by phosphorylation was clearly higher than that of the untreated extraction residue. The phosphorus content of the P-C (34.2 mg P/g) was clearly higher than that of the P-SS (4.6 mg P/g), which indicated that cellulose had larger number of phosphorylation sites than starch, although these were the same group of glucans with different bondings. The total carbon and total nitrogen content of the untreated sample (sago starch-extraction residue, microcrystalline cellulose, and sago starch) and the phosphorylated sample (P-SR, P-C, and P-SS) were nearly identical; there was no significant change during phosphorylation reaction in carbon and nitrogen content. The theoretical phosphate ester percentage for phosphorylated samples was calculated using the carbon and phosphate content. The theoretical phosphate ester percentage for phosphorylated samples means the percentage of the moles of phosphate in phosphorylated sample to the moles of available hydroxyl groups in glucose units. Each glucose unit in starch and cellulose have three moles of available hydroxyl groups and six moles of carbon atoms. The phosphate ester percentage by phosphorylation presented in P-SR, P-C, and P-SS (Table I) was 6.1, 6.3, and 0.9%, respectively.

Infrared microspectrometric characteristics of starch and fiber in P-SR

Micrographic observation focused by FT/IR-4100 type A and IRT-3000 is shown in Figure 1. It was

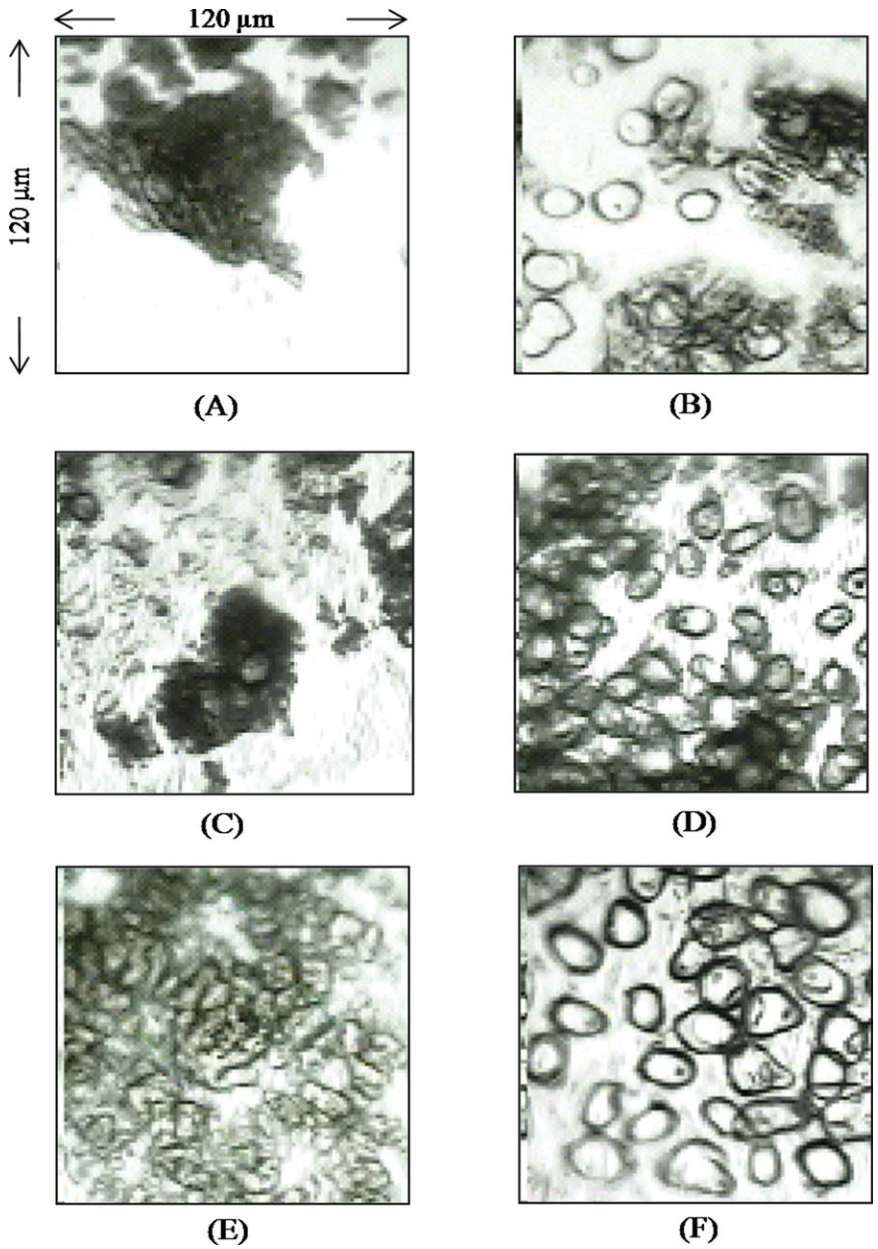

Figure 1 Micrograph of the sago starch-extraction residue [fiber (A) and sago starch (B)], the P-SR [fiber (C) and sago starch (D)], P-C (E), and P-SS (F) (120 μm ×120 μm). P-SR, phosphorylated sago starch-extraction residue; P-C, phosphorylated cellulose; P-SS, phosphorylated sago starch. Each micrograph was obtained using IRT-3000 that could choose the micro area on samples for FT-IR analysis. [Color figure can be viewed in the online issue, which is available at wileyonlinelibrary.com]

observed that fiber cluster (about 60 μm × 90 μm) of sago starch-extraction residue was commonly seen. Sago starch particles presented in sago starch-extraction residue and some starch particles stuck to the fiber [Fig. 1(B)]. The appearance of the fiber and the sago starch in P-SR [Fig. 1(C,D)] was similar to the untreated extraction residue [Fig. 1(A,B)]. These sago starch particles (about 15 μm × 20 μm) in this study were slightly smaller than the ordinary sago starch particles (30–45 μm).

FT-IR analysis of the fiber and the sago starch in the untreated extraction residue and the P-SR were conducted individually. The FT-IR spectra of the untreated sample (sago starch-extraction residue, microcrystalline cellulose, and sago starch) and the phosphorylated sample (P-SR, P-C, and P-SS) are shown in Figures 2 and 3. The FT-IR spectra of all samples showed the large adsorption bands at 3400 cm^{-1} (O—H stretching), 2900–2980 cm^{-1} (C—H stretching), and 1150 and 1070 cm^{-1} (C—O stretching). The FT-IR spectra of fiber fraction in P-SR and P-C [Fig. 3(A,C)] showed new bands at 1750 cm^{-1} [ester carbonyl group (C=O)], 1240 cm^{-1} corresponding to the P=O bonds,[34] and a shoulder at

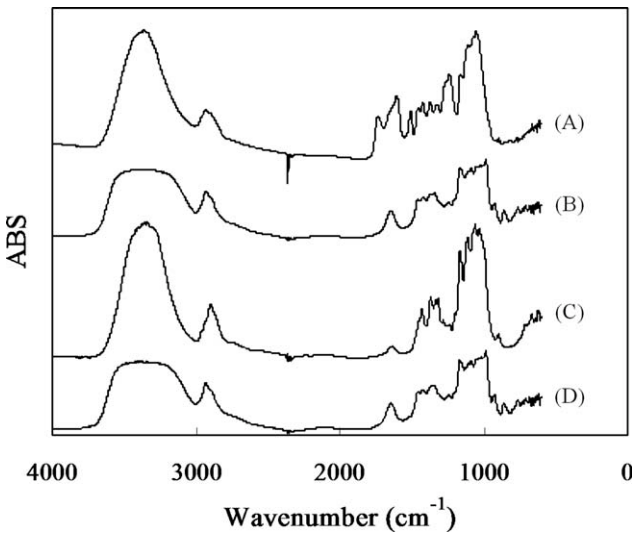

Figure 2 FT-IR spectra of the untreated sago starch-extraction residue [fiber (A) and sago starch (B)], the microcrystalline cellulose (C), and the sago starch (45 μm) (D). Fiber: the fiber in sago starch-extraction residue that mainly consists of cellulose and hemicellulose.

980 cm^{-1} attributed to C—O—P stretching,[35] compared with that of fiber fraction in the untreated extraction residue and microcrystalline cellulose [Fig. 2(A,C)]. On the other hand, the FT-IR spectra of sago starch fraction in P-SR and P-SS [Fig. 3(B,D)] did not show clear change compared with that of sago starch fraction in untreated extraction residue and the sago starch [Fig. 2(B,D)]. The intensities of the bands at 1200 and 980 cm^{-1}, which corresponds to the P=O bonds and C—O—P stretching were compared to those of the untreated extraction residue using the relative absorbance method.[21] The relative absorbance of the bands at 1200 and 980 cm^{-1} for the fiber in untreated extraction residue and P-SR were 1.20 and 0.94 before the phosphorylation and 1.89 and 1.41 after the phosphorylation (Table II). Meanwhile, the relative absorbances for the sago starch in untreated extraction residue and P-SS were nearly same value. Therefore, it is confirmed that the fiber in untreated extraction residue was easily phosphorylated by phosphorylation. Similarly, the relative absorbance of the bands at 1200 and 980 cm^{-1} for P-C was increased by phosphorylation but the relative absorbance for P-SS was maintained. When phosphorylation was occurred on sago starch, phosphorus content of P-SS was clearly lower than that of P-C. Therefore, similar FT-IR spectra for sago starch in the untreated extraction residue and P-SR will be related to the lower amount of phosphorus contents in sago starch.

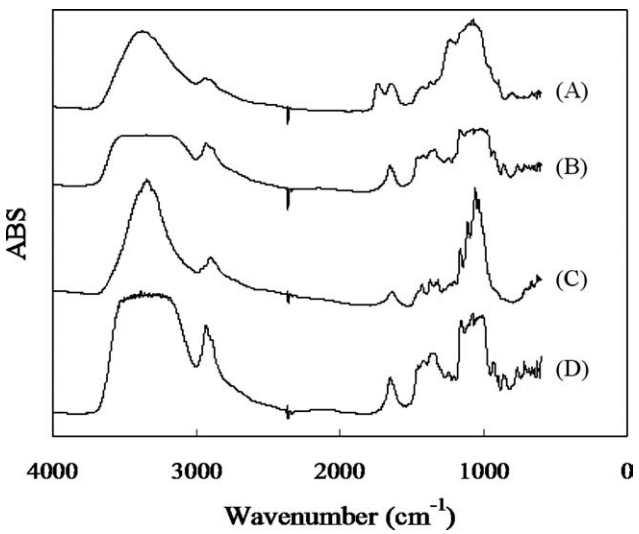

Figure 3 FT-IR spectra of the P-SR [fiber (A) and sago starch (B)], the P-C (C), and the P-SS (D). P-SR, phosphorylated sago starch-extraction residue; P-C, phosphorylated cellulose; P-SS, phosphorylated sago starch.

^{31}P and ^{13}C solid-state NMR spectra of P-SR

Figure 4 shows the ^{31}P solid-state NMR spectrum of the untreated and phosphorylated samples. The ^{31}P solid-state NMR spectrum of the untreated extraction residue did not show any clear peaks, whereas the spectrum of P-SR showed a clear peak in the range of 0–1.0 ppm [Fig. 4(A,B)]. This chemical shift is typical for phosphoric di- and triesters, [36] and thus confirmed the presence of the phosphoric ester in P-SR. The ^{31}P solid-state NMR spectrum of P-SS showed a little peak in the range of 0–1.0 ppm [Fig. 4(E,F)], whereas the spectrum of P-C showed a strong peak in the range of 0–1.0 ppm as chemical shift of typical for phosphoric di- and triesters (Note that the symmetrical side bands at ± 60 ppm are rotational side bands resulting from powder

TABLE II
Relative Absorbance of C—O—P Bonds for Untreated and Phosphorylated Samples

Sample	Relative absorbance[a] 1200 cm^{-1}/ 1325 cm^{-1}	980 cm^{-1}/ 1325 cm^{-1}
Fiber in untreated[b]	1.20	0.94
Fiber in P-SR[c]	1.89	1.41
Sago starch in untreated	0.88	1.25
Sago starch in P-SR	0.86	1.34
Microcrystalline cellulose	0.84	1.23
P-C[d]	1.67	1.45
Sago starch[e]	0.82	1.33
P-SS[f]	0.83	1.36

[a] Band intensity of C—O—P group/band intensity at 1325 cm^{-1}.
[b] The untreated sago starch-extraction residue.
[c] Phosphorylated sago starch-extraction residue.
[d] Phosphorylated microcrystalline cellulose.
[e] The sago starch that was passed through a 45-μm sieve.
[f] Phosphorylated sago starch.

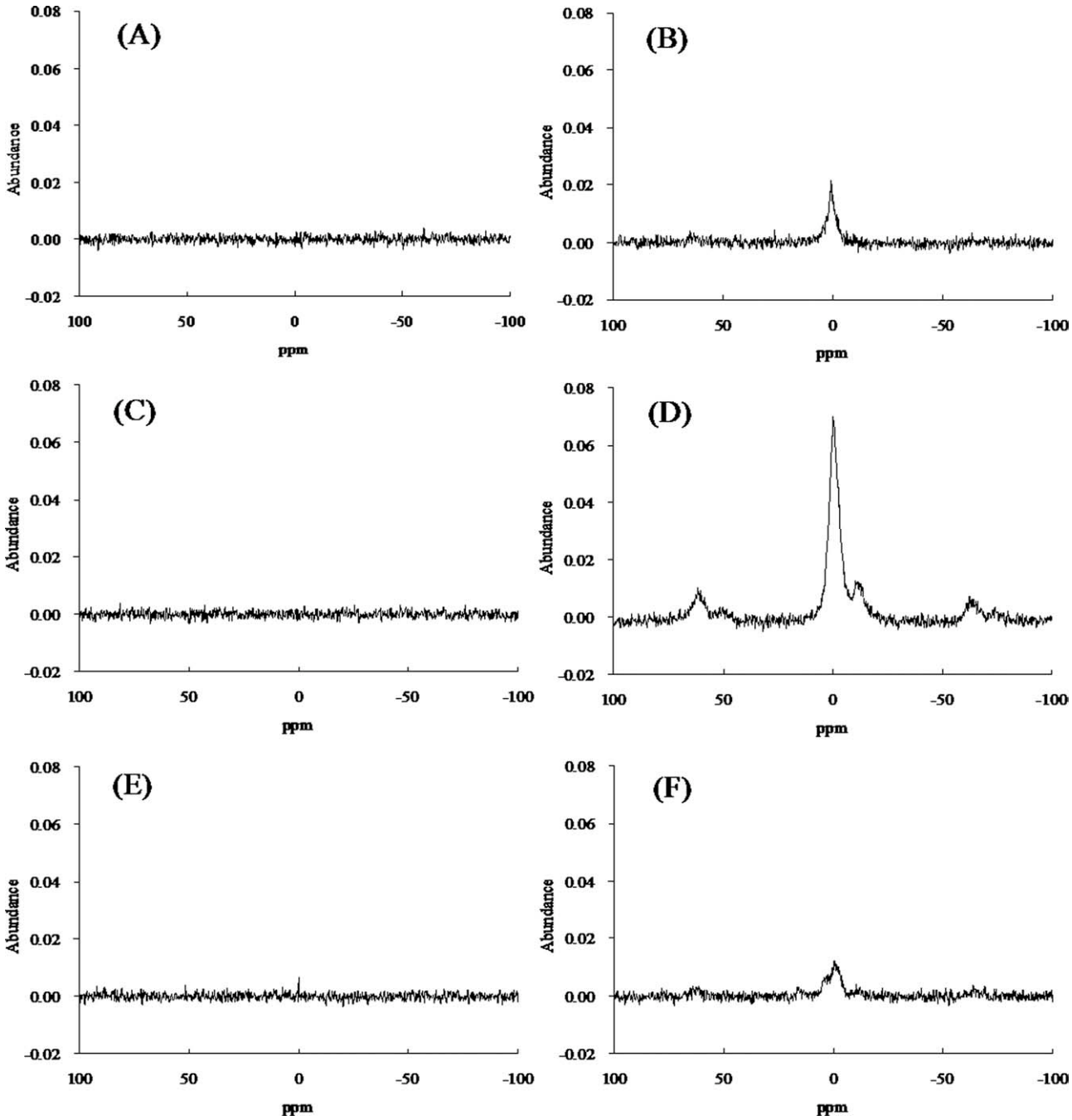

Figure 4 ^{31}P solid-state NMR spectra for the untreated and phosphorylated samples. (A) The untreated sago starch-extraction residue, (B) P-SR, (C) the microcrystalline cellulose, (D) P-C, (E) the sieved sago starch, and (F) P-SS. Untreated: the untreated sago starch-extraction residue, microcrystalline cellulose and the sieved sago starch. P-SR, phosphorylated sago starch-extraction residue; P-C, phosphorylated cellulose; P-SS, phosphorylated sago starch. Standard material of the phosphate: Ammonium phosphate dibasic [$(NH_4)_2HPO_4$].

anisotropy.)[35] [Fig. 4(C,D)]. The resonance of phosphate introduced by phosphorylation was clearly found by NMR, which indicated the sorption sites for heavy metal ions.

The ^{13}C solid-state NMR spectrum of the untreated extraction residue showed four major peaks, at 61.9 (C6), 72.5 (C2, C3, and C5), 82.9 (C4), and 100–103 ppm (C1) [Fig. 5 (A) and Table III].[35,37,38]

These NMR spectra were similar to that of the sago starch and cellulose [Fig. 5(C,E)], because the untreated extraction residue consists of sago starch, cellulose, and hemicellulose. The ^{13}C solid-state NMR spectrum of the P-SR also showed four major peaks [Fig. 5(B)], but the values of chemical shifts were slightly changed (Table III). After the phosphorylation, the chemical shifts of C2, C3, and C6

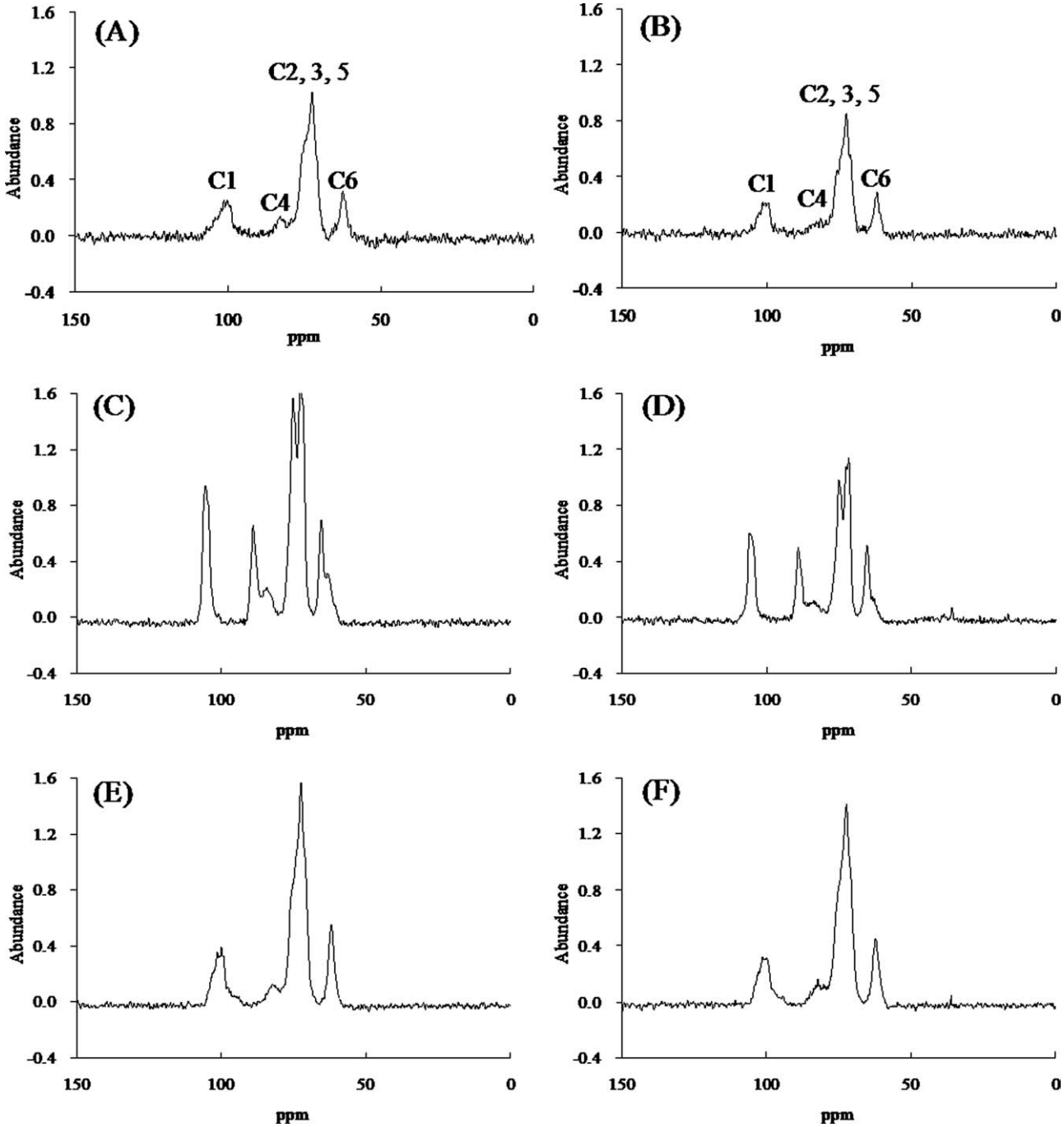

Figure 5 ^{13}C solid state NMR spectra for the untreated and phosphorylated samples. (A) The untreated sago starch-extraction residue, (B) P-SR, (C) the microcrystalline cellulose, (D) P-C, (E) the sieved sago starch, and (F) P-SS. Untreated: the untreated sago starch-extraction residue, microcrystalline cellulose and the sieved sago starch. P-SR, phosphorylated sago starch-extraction residue; P-C, phosphorylated cellulose; P-SS, phosphorylated sago starch. Standard material of the phosphate: Adamantane ($C_{10}H_{16}$). 99.8–103.1 ppm: C1, 83.1 ppm: C4, 72.6 ppm: C2, 3, 5, 62.3 ppm: C6.

(carbons bearing hydroxyl groups) moved to a lower resonance region by β-effect as substitution effect.[35,39] On the other hand, the chemical shifts of C1 and C4 (the glycosidic linkage) of P-SR moved to a higher resonance region by the γ-effect as steric effect,[39] which indicates a modification at C2 or C3 (next to C1 and C4, respectively).

The ^{13}C solid-state NMR spectrum of P-SS showed four major peaks, at 62, 72, 82, and 100–101 ppm [Fig. 5(F)]. These peaks were similar to that of the sago starch. For the P-SS, phosphorus content was lower than that of P-C and P-SR, and the ^{31}P solid-state NMR spectrum peaks for phosphoric di- and triesters were also smaller than that of P-C and

TABLE III
Chemical Shifts of ^{13}C Solid-State NMR Spectra for P-SR

Sample	Chemical shift (ppm)			
	C1	C2, 3, 5	C4	C6
Untreated[a]	102.7, 100.7	72.5	82.9	61.9
P-SR[b]	101.8, 100.4	75.4, 72.7	82.2	62.5
Microcrystalline cellulose	105.5	75.2, 72.8	89.2, 83.2	65.5, 63.1
P-C[c]	105.5, 104.6	75.2, 72.3	89.1	65.7
Sago starch[d]	101.4, 100.1	72.6	82.9	62.4
P-SS[e]	101.2, 100.1	72.6	82.3	62.6, 61.9

[a] The untreated sago starch-extraction residue.
[b] Phosphorylated sago starch-extraction residue.
[c] Phosphorylated microcrystalline cellulose.
[d] The sago starch that was passed through a 45-μm sieve.
[e] Phosphorylated sago starch.

P-SR. Therefore, it seemed that the phosphate ester was hardly formed in the P-SS and the sago starch fraction in P-SR. Cereal starches are generally composed of two crystalline polysaccharides, amylose and amylopectin. Both contain C4-linked α-D-glucopyranose units with double helix structure. Amylose is linear polymer with 200–1000 glucose unit, whereas amylopectin is highly branched, since 5–6% of the C4-linked units are also C6-linked[40] with molecular weight of hundred thousands. It seemed that the lower phosphorus contents of P-SS may be related to the steric hindrance caused by the cluster structure of amylopectin.[41–43] On the other hand, P-C showed the higher phosphorus content, and the ^{31}P solid-state NMR spectrum peaks for phosphoric di- and triesters were strong. The molecular structure of cellulose as a carbohydrate polymer comprises of repeating β-D-glucopyranose units that are covalently linked through acetal functions between the hydroxyl group of the C4 and C1 carbon atoms (β-1,4-glucan).[44] The esterification of the cellulose is hardly influenced by the polarity of hydroxyl group in glucose residues and by the difference in various esterification reactions, thus it gives the high substitution product.[45] The steric hindrance of the β-D-glucose is smaller than that of α-D-glucose, because the hydroxyl group of β-D-glucose is equatorial orientation.[46] The changes of the ^{13}C solid-state NMR spectrum for the P-C from the untreated microcrystalline cellulose [Fig. 5(C,D)] were similar to that of P-SR (Table III). Thus, it seemed that the phosphorylation was easily carried out on fiber as cellulose and hemicellulose in untreated extraction residue compared with the sago starch in that.

Heavy metal sorption characteristics on P-SR

Cadmium sorption on P-SR, P-C, and P-SS

Figures 6 and 7 show the cadmium sorption behavior on P-SR, P-C, and P-SS and that of the maximum sorption capacity (Q_{max}). The amount of sorbed cadmium of P-SR and P-C increased with the increase in equilibrium concentration (Fig. 6), and the Q_{max} of cadmium on P-SR (0.22 mmol/g) and P-C (0.22 mmol/g) was almost the same value. On the other hand, P-SS did not show the increase in the amount of sorbed cadmium with increasing equilibrium concentration. P-SS was not fitted to a

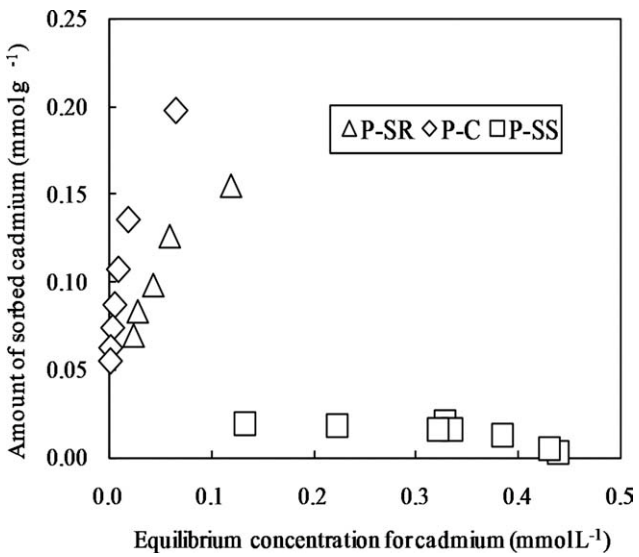

Figure 6 Cadmium sorption behavior on P-SR, P-C, and P-SS. P-SR, phosphorylated sago starch-extraction residue; P-C, phosphorylated cellulose; P-SS, phosphorylated sago starch.

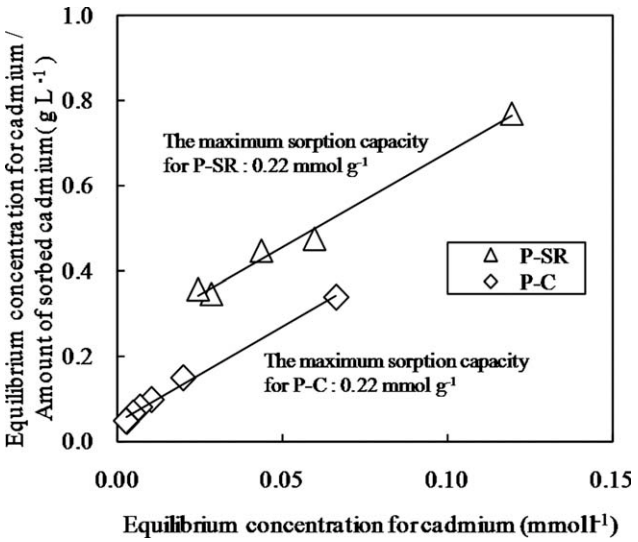

Figure 7 Maximum sorption capacity of cadmium on P-SR, P-C, and P-SS. P-SS was not fitted to a Langmuir isotherm, so that the maximum sorption capacity of cadmium on P-SS was deleted in this figure. P-SR, phosphorylated sago starch-extraction residue; P-C, phosphorylated cellulose.

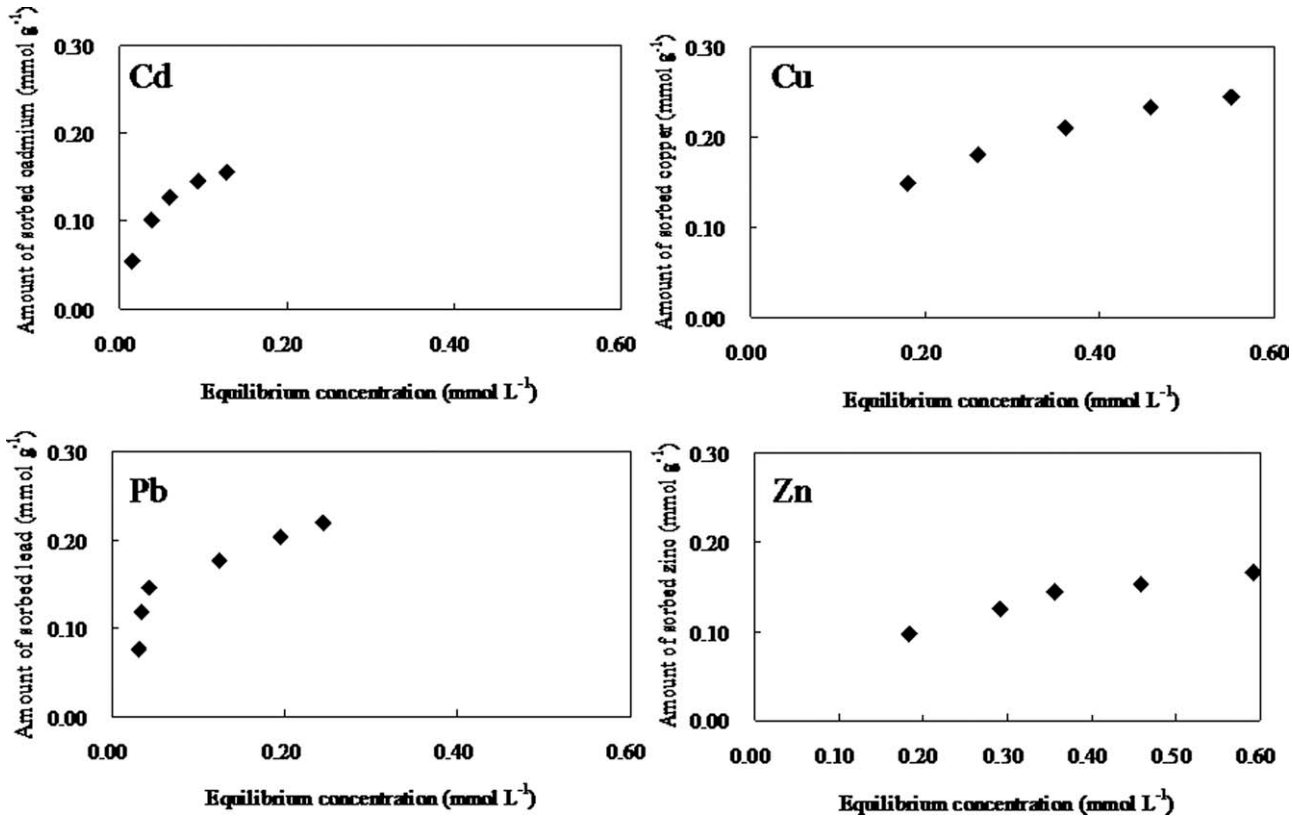

Figure 8 The single heavy metal sorption behavior of cadmium, lead, copper, and zinc on P-SR.

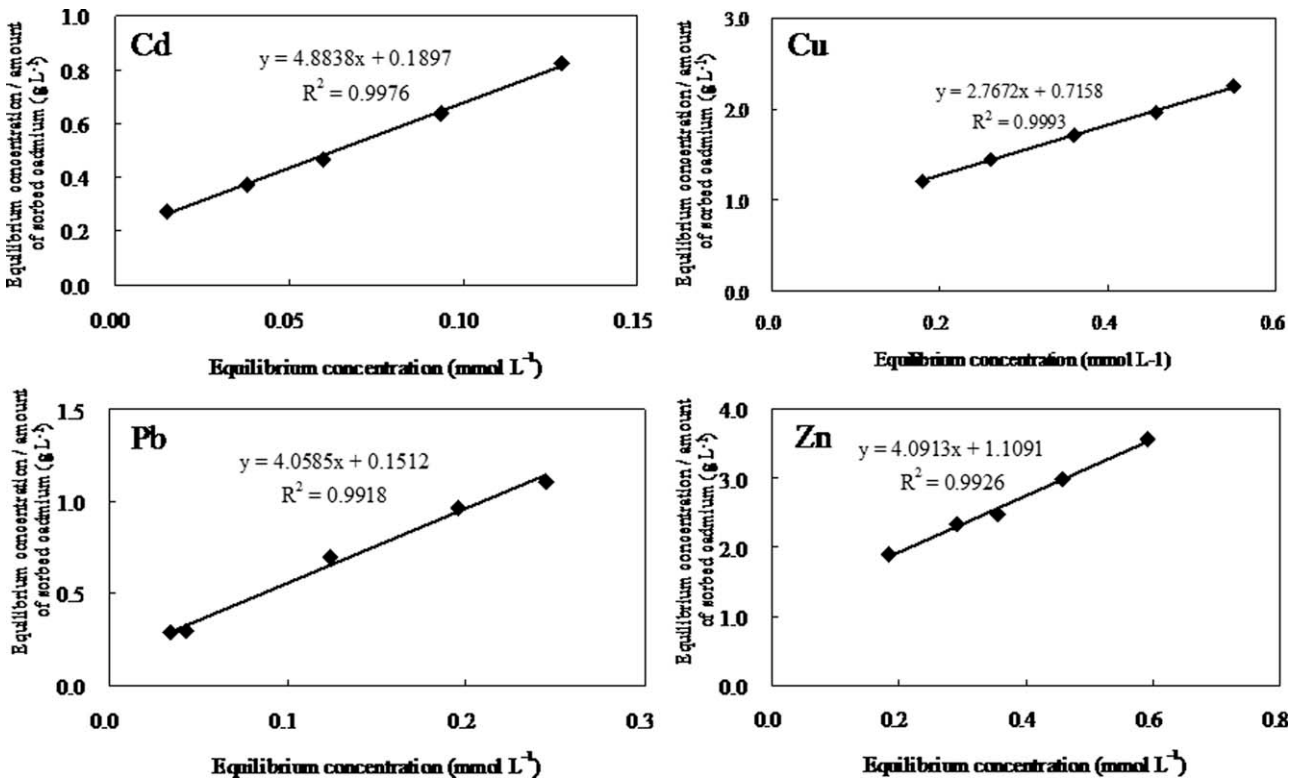

Figure 9 Langmuir isotherm for the sorption of cadmium, lead, copper, and zinc on P-SR.

TABLE IV
Maximum Sorption Capacity of Individual Heavy Metal (cadmium, lead, copper, and zinc) for P-SR

	Maximum sorption capacity	
	mg/g	mmol/g
Cd	23.01	0.20
Pb	51.05	0.25
Cu	22.97	0.36
Zn	15.97	0.24

Langmuir isotherm, so that the data of P-SS on cadmium sorption were deleted from Figure 6. Phosphorus contents of P-SR, P-C, and P-SS were 31.7, 34.2, and 4.6 mg P/g, respectively, (Table I). Phosphorus content of P-SS was clearly lower than that of P-SR and P-C. Therefore, the lower cadmium sorption on P-SS will be related to the lower amount of phosphorus content and phosphate ester in it.

Selectivity for the heavy metal sorption on P-SR

Maximum sorption capacity for individual heavy metal (cadmium, lead, copper, and zinc) on P-SR. Figure 8 shows the single heavy metal sorption behavior of cadmium, lead, copper, and zinc on P-SR. When equilibrium concentration of each heavy metal increased, the amount of sorbed metal ions tended to increase, and each heavy metal finally reached the sorption equilibrium. Figure 9 shows the Langmuir isotherm for the sorption of cadmium, lead, copper, and zinc on P-SR. The Q_{max} of heavy metals (cadmium, lead, copper, and zinc) on P-SR were 0.20, 0.25, 0.36, and 0.24 mmol/g, respectively, (Table IV). The Q_{max} (in mmol/g) of each heavy metal on P-SR followed the order of Cu > Pb > Zn > Cd. The Q_{max} of copper was the highest among four heavy metals. On the other hand, several kinds of organic acid such as fulvic acid show the heavy metal sorption behavior on it. Selectivity sequence for heavy metal cations (Cu, Pb, Zn) on P-SR was similar to that on fulvic acid.[47]

Sorption behavior of coexisted heavy metals on P-SR. Table V shows the amount of sorbed heavy metals on P-SR in coexisted heavy metal solution. The amount of sorbed cadmium, lead, copper, and zinc were 0.039, 0.083, 0.057, and 0.023 mmol/g (39, 83, 57, and 23 μmol/g), respectively. The amount of sorbed heavy metals followed the order of Pb > Cu > Cd > Zn. This result was different from the relations of maximum sorption capacities for individual heavy metals. Nada et al.[16–18] evaluated heavy metals sorption affinity of phosphorylated plant residues (rice straw, bagasse cotton stalk, wood pulp) using the solution that contained several kinds of heavy metals, and the heavy metal sorption affinity was different in every phosphorylated materials such as bagasse (Cu > Pb > Cd > Zn) (the amount of sorbed heavy metals were 12.0, 6.8, 6.4, and 4.0 μmol/g), wood pulp (Cu > Pb > Cd > Zn) (13.4, 8.3, 8.1, and 6.7 μmol/g),[17] rice straw (Cu > Zn > Pb > Cd) (6.3, 3.8, 3.5, and 2.9 μmol/g), and cotton stalk (Cu > Zn > Pb > Cd) (6.1, 4.6, 3.8, and 3.1 μmol/g).[16] The amount of sorbed heavy metals of P-SR was higher than that of these phosphorylated materials, and moreover, the heavy metal sorption behavior of P-SR was clearly different. The sorption affinity varies, depending of the ionic radius and the electro positive charge on the ions.[48] Also, sorption of metals onto the ion-exchanger can be attributed to the intrinsic sorption and Coulombic interaction.[18] The Coulombic force results from the electrostatic energy of interactions between the adsorbents and adsorbate. The charges on the substrates, as well as the softness and hardness of the charge on both side, are mostly responsible for the amount of adsorption. On the other hand, it seemed that the amount of sorbed heavy metal related to the phosphorus content of phosphorylated fiber and starch fractions in P-SR, and the mixture of phosphorylated fiber and starch fractions in P-SR may relate to the selective sorption of heavy metals on it.

CONCLUSION

By phosphorylation, the phosphate ester was introduced into sago starch-extraction residue. The phosphorus content of P-SR was almost the same as that of P-C, and P-SS showed the lowest phosphorus content in all phosphorylated products. The presence of the phosphoric ester in P-SR, P-C, and P-SS was confirmed by infrared microspectrometric analysis and solid-state NMR analysis, but each spectrum of P-SS was not clear compared with P-SR and P-C. The phosphate ester percent of P-SR, P-C, and P-SS by phosphorylation was 6.1, 6.3, and 0.9%, respectively.

The cadmium sorption on P-SR and P-C were higher than P-SS. It seemed that the difference of the amount of sorbed heavy metal on phosphorylated products related to the amount of phosphorus

TABLE V
The Amount of Sorbed Heavy Metals on P-SR in Mixed Heavy Metal Solution

	The amount of sorbed heavy metal	
	mg/g	mmol/g
Cd	4.35	0.039
Pb	17.12	0.083
Cu	3.60	0.057
Zn	1.50	0.023

The mixed heavy metal solution contained the 0.2 mol/L of cadmium, lead, copper, and zinc, respectively.

content in it. Then, almost all of phosphate ester was formed on the fiber in P-SR.

In single heavy metal sorption on P-SR, the maximum sorption capacities of heavy metals (cadmium, lead, copper, and zinc) on P-SR were 0.20, 0.25, 0.36, and 0.24 mmol/g (Cu > Pb > Zn > Cd), respectively. On the other hand, the amount of sorbed heavy metals in coexisted heavy metal sorption on P-SR followed the order of Pb > Cu > Cd > Zn. Thus, the heavy metal sorption behavior in single and coexisted heavy metal solution for P-SR were different, and it is suggested that P-SR had the intrinsic sorption affinity for heavy metals.

The authors are grateful to Professor Emeritus Ryunosuke Hamada, Tokyo University of Agriculture and Technology, for critical review.

References

1. The Official Journal of the European Communities, EUR-OP, Luxembourg, 1998.
2. National Recommended Water Quality Criteria for Priority Pollutants, Environmental Protection Agency, United States, 2009.
3. Basic Environment Act, Ministry of the Environment, Tokyo, Japan, 1993.
4. Guidelines for drinking-water quality, Vol. 1, 3rd edition incorporating 1st and 2nd addenda, World Health Organization, 2008.
5. Lee, M.; Paik, I. S.; Kim, I.; Kang, H.; Lee, S. J Hazard Mater 2007, 144, 208.
6. Pehlivan, E.; Altun, T. J Hazard Mater 2007, 140, 299.
7. Rengaraj, S.; Yeon, K. H.; Kang, S. Y.; Lee, J. U.; Kim, K. W.; Moon, S. H. J Hazard Mater 2002, B92, 185.
8. Abo-Farhaa, S. A.; Abdel-Aala, A. Y.; Ashourb, I. A.; Garamona, S. E. J Hazard Mater 2009, 169, 190.
9. Babel, S.; Kurniawan, T. A. J Hazard Mater 2003, B97, 219.
10. Bayat, B. J Hazard Mater 2002, B95, 251.
11. Ritchie, S. M. C.; Bhattacharyya, D. J Hazard Mater 2002, 92, 21.
12. Lee, H.; Yang, J. J Hazard Mater 2000, B77, 227.
13. Kumar, U.; Bandyopadhyay, M. Bioresour Technol 2006, 97, 104.
14. Johns, M. M.; Marshall, W. E.; Toles, C. A. J Chem Technol Biotechnol 1998, 71, 131.
15. Karim, A. A.; Pei-Lang Tie, A.; Manan, D. M. A.; Zaidul, I. S. M. Compr Rev Food Sci Food Safety 2008, 7, 215.
16. Nada, A. M. A.; Eid, M. A.; El Bahnasawy, R. M.; Khalifa, M. N. J Appl Polym Sci 2002, 85, 792.
17. Nada, A. M. A.; Eid, M. A.; Sabry, A. I.; Khalifa, M. N. J Appl Polym Sci 2003, 90, 97.
18. Nada, A. M. A.; Hassan, M. L. J Appl Polym Sci 2003, 89, 2950.
19. Igura, M.; Okazaki, M.; Kimura, S. D.; Toyota, K.; Ohmi, M.; Kuwabara, T.; Syuno, M. Sago Palm 2007, 15, 1.
20. Ohmi, M.; Inomata, H.; Sasaki, S.; Tominaga, H.; Fukuda, K. Sago Palm 2003, 11, 1.
21. Igura, M.; Okazaki, M. J Hazard Mater 2010, 178, 686.
22. Yadanaparthi, S. K. R.; Graybill, D.; Wandruszka, R. V. J Hazard Mater 2009, 171, 1.
23. Saito, N.; Aoyama, M. J Hokkaido Forest Products Res Inst 1991, 5, 15.
24. Strelko V. Jr., Streat, M.; Kozynchenko, O. React Funct Polym 1999, 41, 245.
25. Terada, S.; Ueda, N.; Kondo, K.; Takemoto, K. Kobunshi Kagaku 1972, 29, 500.
26. Ghimire, K. N.; Inoue, K.; Makino, K.; Miyajima, T. Water Res 2003, 37, 4945.
27. Kim, S.-H.; Song, H.; Nisola, G. M.; Ahn, J.; Galera, M. M.; Lee, C. H.; Chung, W.-J. J Ind Eng Chem 2006, 12, 469.
28. Watanabe, T.; Ohmi, M. Sago Palm 1997, 5, 10.
29. Tsujimoto, M.; Akiyama, N.; Okazaki, M.; Nakata, M. Sago Palm 2008, 16, 53.
30. Nanjyo, M. Analytical Methods of Soil Environment; Hakuyusya: Tokyo, 1997.
31. Murphy, J.; Riley, J. P. Anal Chim Acta 1962, 27, 31.
32. Yamada, H. Analytical Methods of Soil Environment; Hakuyusya: Tokyo, 1997.
33. Asashima, M.; Miyama, S. Fresh Water and the Marine Environment; Maruzen Co. Ltd.: Tokyo, Japan, 2009.
34. Suflet, D. M.; Chitanu, G. C.; Popa, V. I. React Funct Polym 2006, 66, 1240.
35. Granja, P. L.; Pouysegu, L.; Petraud, M.; De Jeso, B.; Baquey, C.; Barbosa, M. A. J Appl Polym Sci 2001, 82, 3341.
36. Tebby, J. C. CRC Handbook of Phosphorus-31 Nuclear Magnetic Resonance Data; CRC Press: Florida, 1991.
37. Zhang, X.; Golding, J.; Burgar, I. Polymer 2002, 43, 5791.
38. Okazaki, M.; Igura, M.; Kimura, S. D.; Lina, S. B.; Matsumura, S.; Nakato, T.; Takahashi, K.; Quevedo, M. A.; Loreto, A. B. Developing Processes of Sago Starch Structure; TUAT Press: Tokyo, Japan, 2008.
39. Hoshino, M.; Takai, M.; Fukuda, K.; Imura, K.; Hayashi, J. J Polym Sci Part A: Polym Chem 1989, 27, 2083.
40. Morgan, K. R.; Furneaux, R. H.; Larsen, N. G. Carbohydr Res 1995, 276, 387.
41. Morgan, K. R.; Furneaux, R. H.; Stanley, R. A. Carbohydr Res 1992, 235, 15.
42. Manners, D. J.; Matheson, N. K. Carbohydr Res 1981, 90, 99.
43. Gidley, M. J.; Bociek, S. M. J Am Chem Soc 1985, 107, 7040.
44. O'Connell, D. W.; Birkinshaw, C.; O'Dwyer, T. F. Bioresour Technol 2008, 99, 6709.
45. Isogai, A. Cellulose Science; Asakura Publishing Co., Ltd: Tokyo, 2003.
46. Kondo, Y. J Food Sci 1994, 49, 15.
47. Schnitze, M.; Hansen, E. H. Soil Sci 1970, 109, 333.
48. Reddad, Z.; Gerente, C.; Andres, Y.; Cloirec, P. L. Environ Sci Technol 2002, 36, 2067.